J Mater Sci (2007) 42:4824–4831
DOI 10.1007/s10853-006-0734-z

Piezoelectric hydrophones from optimal designs, Part I: fabrication

Christopher J. Reilly · John W. Halloran · Emilio C. N. Silva

Received: 1 December 2005 / Accepted: 28 July 2006 / Published online: 16 March 2007

Abstract Complex three-dimensional optimal designs for improved piezoelectric hydrophones were being realized in lead zirconate titanate piezoelectric ceramics using an indirect solid freeform fabrication technique employing lost molds to define internal void spaces. Lost molds were fabricated by wax-based ink jet deposition, and replicated in PZT ceramic using acrylate suspension polymerization. The physical size of the object is determined by the finest feature present in the design, and by the resolution of the ink jet device. Arrays with 125 repeat units were fabricated with a fidelity of 0.9% in placement of features. The Indirect Solid Freeform Fabrication technique is described in detail.

Introduction

Recently optimal design techniques have used computational optimal design methods using the Topology Optimization and Homogenization algorithm [1] has been used to design piezoelectric composites with elastic and piezoelectric coefficients optimized for hydrophone transducers [2–5]. Two-dimensional versions of these were recently fabricated from PZT by a co-extrusion method, and showed outstanding performance in close agreement to design predictions [6]. This paper considers three-dimensional designs, which are fabricated by casting into molds defined by solid freeform fabrication. A companion paper will present the evaluation of the properties and comparison with expectations from the design.

C. J. Reilly · J. W. Halloran (✉)
Department of Materials Science and Engineering, University Of Michigan, 3062 Dow Building, Ann Arbor, MI 48109-2136, USA
e-mail: john_halloran@engin.umich.edu

E. C. N. Silva
Department of Mechatronics and Mechanical Systems Engineering, Escola Politécnica, University of São Paulo, Sao Paulo, Brazil

Piezocomposites and hydrophones

The relationship between the induced polarization and the applied stress is expressed by the third-rank tensor of piezoelectric coefficients, d_{ijk} units of picocoloumbs per Newton (pC/N). For the case of a hydrostatic stress state, we consider the hydrostatic piezoelectric response d_h of material is the sum of the piezoelectric terms from all three directions simultaneously,

$$d_h = d_{33} + d_{13} + d_{23}$$

The net hydrostatic response of a block of piezoelectric PZT is roughly negated [7, 8] by the equal but opposite contributions from d_{33} and $(d_{13} + d_{23})$. Thus solid blocks of PZT have a relatively poor d_h values. A hydrophone transducer is employed as a sensor, and its sensitivity is determined by the voltage produced in response to a hydrostatic pressure wave. The hydrostatic voltage coefficient, g_h, relates the measured voltage to an applied hydrostatic stress. The g_h and d_h terms are related by the relative permittivity of the material K and ε_o the permittivity of free space,

$$g_h = \frac{d_h}{\varepsilon_o K}$$

A useful figure of merit for a hydrophone transducer is the product of the hydrostatic piezoelectric response d_h and the hydrostatic voltage coefficient g_h, which expresses the hydrophone figure of merit, $d_h g_h$, has units of $m^2\ N^{-1}$.

$$d_h g_h = \frac{d_h^2}{\varepsilon_o K}$$

The hydrophone figure of merit can be increased by designing a transducer that either increases the hydrostatic piezoelectric response, decreases the permittivity or some combination of both. The designs of Silva et al. [3] are aimed at optimizing either the hydrophone voltage coefficient g_h or the combined figure of merit $d_h g_h$.

This paper presents the fabrication method by which these designs were realized in Lead Zirconate Titanate (PZT). This process involves the suspension polymerization casting of a ceramic loaded acrylate monomer solution into a lost mold made by a Solid Freeform Fabrication tool, and is called Indirect Solid Freeform Fabrication (ISFF).

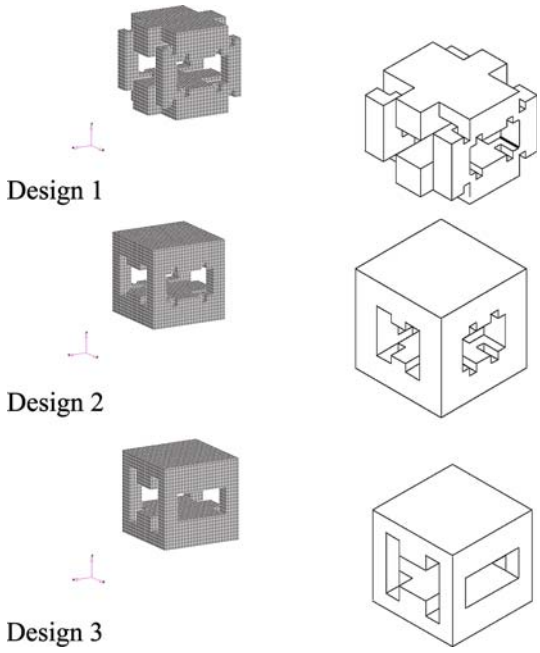

Fig. 1 The voxelated structures output by the Topology Optimization design algorithm are shown on the left. Corresponding images of the designs after translation to solid body CAD files are on the right

Fabrication process overview

The first step is to manually translate the voxelated output of the Topology Optimization algorithm from its Finite Element Model format (Hypermesh, Altair Engineering, Troy, MI) into a solid body Computer Aided Drawing (AutoCAD r14, AutoDesk Inc.) model. In this form, it can undergo Boolean manipulations, be used to form arrays if necessary, and subsequently be further translated into an .stl file. The FEM-CAD transformation is not merely cosmetic, as these CAD functions are important to the overall ISFF process. An .stl file describes the surface boundaries of the part as a series of tessellated triangles, and it is the standard format for file building in the Solid Freeform Fabrication industry. The lost mold that is to be used in the ISFF process must be in .stl format in order to be fabricated by an SFF tool. Also, this lost mold defines the internal void spaces of the part that is to be realized in ceramic, and is a Boolean negative of the original design. Images of the voxelated FEM outputs are shown with their corresponding solid body CAD file images for comparison in Fig. 1.

A brief outline of the Indirect Solid Freeform Fabrication process is shown in Fig. 2. Once the FEM

Step 1. CAD file of design to be fabricated.

Step 2. The Boolean Negative of CAD File is built on the 3d Inkjet Printer to be used as a lost mold.

Step 3. A ceramic loaded acrylate monomer solution is cast and cured in the lost mold to form a 50vol% ceramic/50vol% acrylate part in the desired shape.

Step 4. The green body is put through a controlled heating schedule to burn off the mold and binder leaving a 50vol% ceramic/50vol% air body.

Step 5. The part is sintered to full density at high temperature.

Fig. 2 An overview of the Indirect Solid Freeform Fabrication Process

design is translated to a CAD solid body format, the next step is to make a Boolean negative of the design unit cell. (Step 2) This CAD negative can be formed into an array of unit cells and given a border to define the boundary of the part. Figure 3 is an example of a $3 \times 3 \times 1$ array of unit cells with a wall added to the negative to define the part perimeter. This figure clearly illustrates how the lost mold defines the internal features of the PZT-air piezocomposite structure. The bounded array of negatives is the lost mold, which must be fabricated by a Solid Freeform Fabrication (SFF) tool. This part is translated to an .stl file and sent to the proper software package to prepare the file for building on the SFF tool. For this case, the lost mold is fabricated using a commercial polysulfonamide material (Protobuild^{TM}, SolidScape, Inc., Merrimack NH) using an SFF device employing solid ink jets (ModelMaker II, Sanders Design International, Merriack NH), in which the part is built from many thousands of droplets of molten waxy materials.

Once the mold is made, a 52 vol% PZT loaded acrylate monomer solution is cast into the mold cavity. (Step 3) Suspension rheology is of utmost importance to successful ISFF as the PZT loaded suspension must be fluid enough to flow into and fill all mold features in order to accurately replicate the design. The PZT suspension must also have a high enough solids loading so that after binder removal the part is self supporting and sinterable. With the mold filled, polymerization of the acrylate binder is induced in situ. This entraps the PZT powder in a polymer network to form a 52 vol% PZT/48 vol% acrylate part in the shape of the design, with the mold defining the internal void spaces and perimeter of the piezocomposite. (Step 3) Curing kinetics of the acrylate binder system are characterized in another paper [9]. The cured green body is put through a controlled heating schedule to burn-off the mold and acrylate binder leaving a 52 vol% ceramic/48 vol% air body (Step 4). Finally, the part is sintered to full density at high temperature (Step 5).

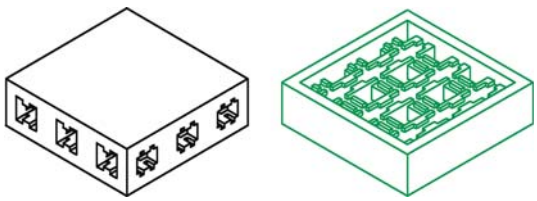

Fig. 3 A $3 \times 3 \times 1$ array of design 2, along with its corresponding Boolean negative mold

Mold fabrication

The mold that is built on the SFF tool is comprised of one or more inverted versions (Boolean negatives) of the original Topology Optimization (TO) algorithm unit cell output. Neither the output of the TO code nor the negative have a physical dimension assigned to them since the algorithm operates in dimensionless voxel space. However, the 3d inkjet printer SFF mold making tool builds objects from primitives with finite size. The relevant ISFF issues pertaining to the coupling of the dimensionless voxels of the design space to the finite primitives of the mold building tool are the subject of this section.

There are many benefits to make the piezoelectric device as small as possible. The removal of the binder system is greatly facilitated when diffusion distances are short. The electric field obtained across the final part will be higher for thinner structures. Unfortunately there is a lower size limit for mold fabrication and it is determined by both the design and the mold building tool. The smallest feature in the design does not possess a dimension, but you can still extract a descriptive ratio from it. For a complex optimally designed hydrophone such as design 2 in Fig. 1, the ratio of the smallest feature to the length of the side is equal to 0.083 or 1/12. For a simple design such as design 5 that ratio would be 0.5. This dimensionless ratio, taken from the design unit cell geometry, is termed gamma (γ) in the following discussion. The design is dimensionless, but the SFF mold making tools used in this work build objects from primitives [10] (G in the following discussion) of finite size. In the SLA it is a string of cured resin (G ~ 300 μm), in the Ink Jet printer it is the splat from two juxtaposed droplets (G ~ 150 μm) and in Fused Deposition Modeling, the primitive is the road of thermoplastic (G ~ 500 μm) coming from the extruder. G is a tool specific parameter equal to the primitive size and gamma is a dimensionless ratio taken from the design geometry. The finest feature in the object being built must be larger than the primitive (G), though preferably twice as large (2G) to preserve the design fidelity. The ratio $2G/\gamma$ determines the physical size of the object. Figure 4 illustrates this by showing the final mold size for a $3 \times 3 \times 3$ array of unit cells of the three designs fabricated on each of the four different SFF tools. Depending on the tool and the design, there can be tremendous variance in final mold size. For example, a $3 \times 3 \times 3$ mold for design 2 fabricated by FDM would have $x = y = z = 36$ mm while a $3 \times 3 \times 3$ mold for design 5 fabricated by a 3d Inkjet Printer would have $x = y = z = 1.8$ mm.

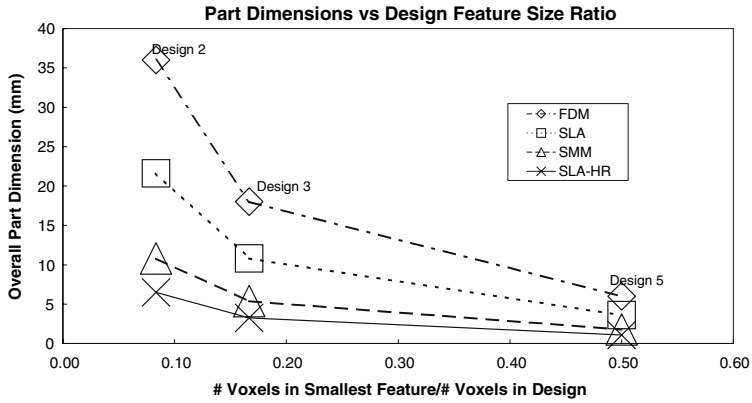

Fig. 4 Final mold size for a $3 \times 3 \times 3$ array of unit cells of the three designs fabricated on each of the four different SFF tools: fused deposition modeling (FDM); Sanders Model Maker (SMM); stereolithography (SLA); and high resolution stereolithography (SLA-HR)

Slurry formulation and rheology

The starting material for use in this acrylate based ISFF process is PZT 586 (American Piezo Ceramics, Mackeyville, PA) powder with median particle size (D_{50}) 1.1 μm, density of the powder is 7.5 g/cm^3 and specific surface area of 0.75 m^2/g. The PZT slurry is formulated from this powder and acrylate monomers with two goals in mind. One is to obtain the lowest possible suspension viscosity to ensure the replication of small mold features during casting. The other, conflicting aim, is to maintain a solids loading sufficient for the cured part to sinter to full density. To achieve the low viscosity and high solids loadings for successful ISFF of the piezoelectric device, it is essential to prepare a stable colloidal dispersion of PZT. A polyelectrolyte surfactant is used to mitigate the interparticle attractions and prevent particle agglomerations from forming. This maintains the fluidity of the slurry even at high solids loadings.

Several different cationic dispersants were evaluated for use with the PZT-acrylate system. The commercial quaternary ammonium acetate Emcol-CC-55 (Goldschmidt, Houston, TX) proved to be the most effective, and its structure is shown in Fig. 5. It should be noted that the PZT586 is a spray dried powder with a Poly Vinyl Alcohol (PVA) based surface coating on the particles. This PVA coating must be removed by heating to 600 °C prior to slurry formulation. Heating caused a 0.9% weight loss and surface area analysis showed an increase from $0.5 \pm .003$ m^2/g before heating to 0.623 ± 0.008 m^2/g after heating. The weight loss and rise in surface area are both consistent with removal of the polymer coating.

The monomer solution used in the formulation of the PZT slurry has three components, one monofunctional acrylate monomers, one difunctional acrylate monomer and a diluent/solvent. Their chemical structures appear in Fig. 5. The acrylate monomers comprise 80 vol% of the monomer solution and are present as a 7:1 mix of Isobornyl Acrylate (IBA, Sartomer 506, Aldrich, Milwaukee, WI) to Propoxylated Neopentyl Glycol Diacrylate (PNGPDA, Sartomer 9003, Aldrich, Milwaukee, WI). This ratio was chosen to provide a low viscosity monomer solution, which cured to make green plastic body strong enough to be easily handled. The remaining 20 vol% is decahydronapthalene (Decalin, Avacado Corp). Decalin is an advantageous addition to the monomer solution premix as it greatly decreases the initial monomer solution viscosity prior to solids loading, and is beneficial to the pyrolysis of the green body due to is relatively high volatility. The low viscosity decalin acts as a diluent in the monomer solution, lowering the viscosity of the monomer solution premix as well as the PZT slurry. To illustrate the utility of the addition of decalin consider the following example. An undiluted 50/50 mix of IBA to PNGPDA has a viscosity of 11 mPa s, but a monomer solution that is 20 vol% decalin has a viscosity of 4.57 mPa s at 25 °C as measured by capillary rheometry (Cannon Fenske ASTM D445). The decalin is entrapped during curing and causes the polymerization of the acrylates to result in a softer solvent swollen gel structure. Thermo Mechanical Analysis measurements by Miao et al. [11] demonstrated that decalin lowers strains during binder pyrolysis, thereby reducing the threat of part cracking. Table 1 lists the physical properties of the components used in the formulation of the monomer solution, prior to the addition of the ceramic powder.

The effect of solids loading on the flow behavior of idealized suspensions of hard spheres has been reviewed by Bergstrom [12]. The dependence of slurry viscosity on the solids loading and initial viscosity of the medium can be modeled by the Kreiger–Dougherty equation[13]

Fig. 5 Chemical Structure of the monomer solution components

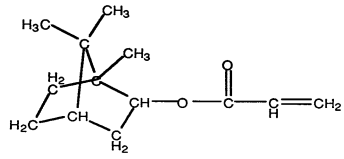

Isobornyl acrylate (IBA)

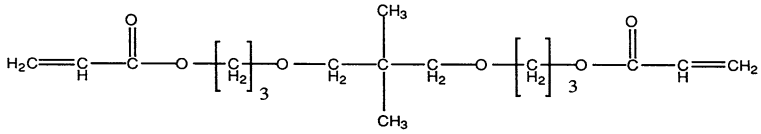

Propoxylated neopentyl glycol diacrylate (PNPGDA)

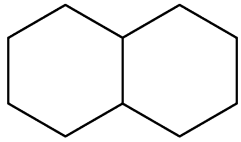

Decahydronaphthalene

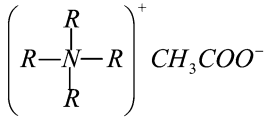

CC-55 Dispersant

Table 1 Physical properties of monomer solution components

Chemical description	Function	Molecular weight (g/mol)	Viscosity (mPa s)
IBA	Mono-functional monomer	208	9
PNGPDA	Difunctional monomer	328	15
Decahydronaphthalene (decalin)	Diluent solvent	138	0.967
CC-55	Dispersant	Unknown	n/a

$$\eta = \eta_o\left(1 - \frac{\beta\phi}{\phi_0}\right)^{-2.5\phi_o}$$

where η is the viscosity of the suspension, η_o is the viscosity of the unloaded liquid, ϕ is the volume fraction of the powder dispersed in the suspension and ϕ_0 is the theoretical maximum packing fraction, typically 0.64 for random close packing of monomodal particles. The term β is the effective packing factor of the powder in the suspension, it represents a deviation from the idealized hard sphere model ($\beta = 1$) wherein flocculated particles have trapped liquid medium, resulting in an increased effective phase volume of ceramic particles and attendant viscosity [14]. The exponent 2.5 is appropriate for spherical particles, although modifications to this term have been used to account for irregularly shaped particles.

Several high volume solids loadings PZT IBA/PNGPDA/Decalin slurries were prepared for rheometry. One initial batch of 60 vol% PZT IBA/PNGPDA/Decalin suspension was formulated and diluted back down to 59, 58, 57, 55, 53, and 52 vol% by mixing in additional monomer solution. The rheological properties of the suspensions were measured by a rheometer with concentric cylinder C14 (Bohlin CS-50, Cranbury, NJ). The slurry was agitated for 10 s at room temperature prior to starting the measurement. The viscosity was measured and recorded as the shear rate was increased.

The viscosity versus shear rate plots PZT slurries are shown in Fig. 6. All exhibit a shear thinning behavior at low shear rates and a Newtonian limit appearing above 10 s^{-1}, which is typical for colloidal particle suspensions. The Newtonian limiting viscosity from the flow curves for the PZT slurries are shown as a function of the solids loading in Fig. 7, along with a Krieger–Dougherty fit to the data with an effective packing factor $\beta = 1.02$. The parameter β provides insight into the effectiveness of the dispersant and the ideality of the slurry. The β value can be used to estimate [15] the

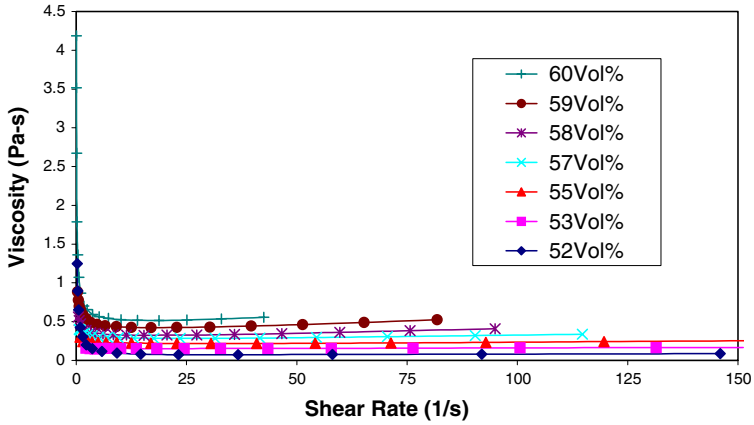

Fig. 6 Viscosity versus shear rate for IBA/PNGPDA/Decalin of various solids loadings PZT with 1 wt% CC-55 dispersant. Testing temperature was 25 °C

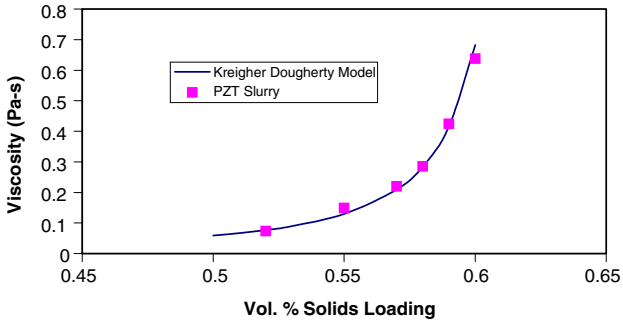

Fig. 7 Newtonian limits of IBA/PNGPDA/Decalin slurries plotted as a function of the solids loading along with a Kreiger–Doughety model fit to the data with an effective packing factor B value B = 1.02

adsorbed layer of dispersant + trapped monomer solution (b) surrounding the ceramic particle of diameter d.

$$\beta = \left(1 + \frac{2b}{d}\right)^3$$

Using $\beta = 1.02$ from the empirical fit of the Kreiger–Dougherty model to the viscometry data for the PZT/IBA/PNGPDA/Decalin slurry gives an adsorbed surfactant layer thickness of $b = 4$ nm. This is the same order of magnitude though slightly lower than values obtained by other researchers [12, 15]. This implies that there is less monomer solution trapped near the particles in this PZT slurry, giving a lower effective phase volume of solids and slurry behavior that is closer to ''hard-sphere'' ideality.

Organic binder removal and sintering

The pyrolysis behavior of the polymerized sample was characterized by the thermogravimetric analysis (TGA) using Cahn TG171 system (Cahn, Madison, WI). An air atmosphere was used and the heating rate was set as 10 °C/min. The data was collected during the heating process. After reaching 600 °C, the instrument was cooled down. The data is plotted in Fig. 8. This plot shows that the acrylate binder system can be completely removed through a simple heating regimen. The TGA records the weight loss of the sample as the temperature increases. It makes apparent the temperature regions of steepest weight loss. To lessen the potential of crack formation, the molded parts are heated slowly in the temperature range mass loss is

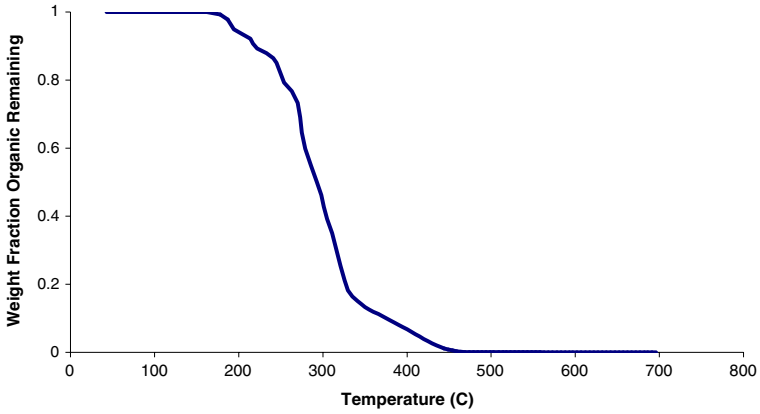

Fig. 8 Thermogravimetric analysis (TGA) of polymerized acrylates showing weight loss and as a function of temperature

most rapid. The addition of decalin to the monomer solution was beneficial to the suspension rheology as discussed earlier. It is also an advantageous aid to the binder burnout process. Miao [11] demonstrated that decalin lowers strains during burnout, thereby reducing cracking. Binder free parts were sealed in an alumina crucible containing 50 vol% PZT + 50 vol% ZrO_2 setter bed powder and heated 5 °C/min to 1,275 °C for 4 h. The setter bed acts as a sacrificial source of lead, which increases the vapor pressure of lead and prevents lead loss from the PZT ceramic during sintering. The density of the PZT was measured using the Archimedes technique to be 98.8% of the manufacturer reported value of 7.5 g/cm^3. The microstructure of a sintered specimen that had been polished and thermally etched (1,200 °C) is pictured in Fig. 9. The PZT ceramic fabricated by ISFF had a final sintered grain size of ~9 microns and a d_{33} of 613 (7 pC/N when poled at 2 kV/mm at 120 °C and measured with a Berlincourt d_{33} tester. The manufacturers specifications list d_{33} for the PZT586 powder to be 620 pC/N. This suggests that the conditions of 2 kV/mm at 120 °C are sufficient to polarize the ceramic.

Results art to part

The ISFF-fabricated PZT parts shown compared with the CAD designs in Fig. 10 for Design 1 and Fig. 11 for Design 2, as a $5 \times 5 \times 5$ arrays with 125 repeat units and a $3 \times 3 \times 1$ arrays with nine repeat units, with minimum feature size of 400 microns. The accuracy of the part fidelity relative to the design was gauged by comparing slice sections of the CAD file to internal sections of a hydrophone specimen made viewable by polishing. The $3 \times 3 \times 1$ array of repeat units of Design 3 was mounted in epoxy and internal cross sections were exposed by grinding through the mounted part

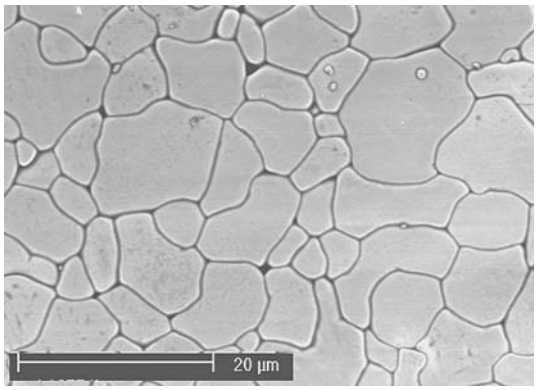

Fig. 9 Microstructure of a sintered specimen fabricated by ISFF that had been polished and thermally etched (1,200 °C)

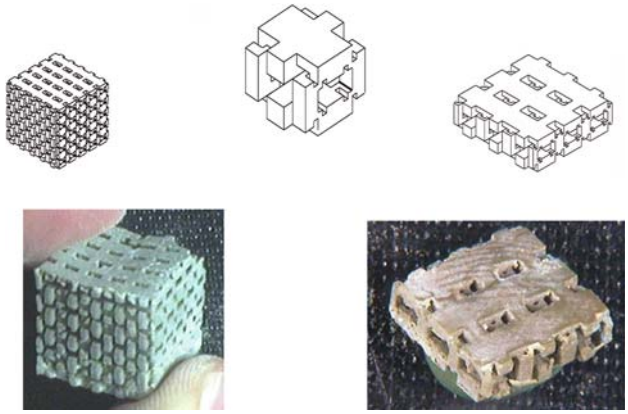

Fig. 10 CAD files of the unit cells of the original design 1 illustrated for comparison along with a $5 \times 5 \times 5$ array (24 mm cube) and $3 \times 3 \times 1$ array (24 mm^2, 8 mm thick) fabricated in PZT with a minimum feature size of 400 micron

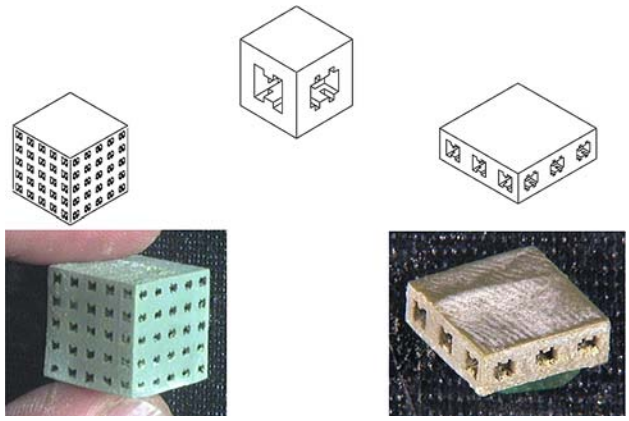

Fig. 11 CAD files of the unit cells of the original design 2 illustrated for comparison along with a $5 \times 5 \times 5$ array (24 mm cube) and $3 \times 3 \times 1$ array (24 mm^2, 8 mm thick) fabricated in PZT with a minimum feature size of 400 microns

along the z-axis. The Density Slice function within NIH Image photographic analysis software was employed to capture the portions of the image of the mounted PZT part that fell within a certain brightness/contrast window. This effectively selected the PZT sections out of the image, separating them from the epoxy used as a sample mount. The software was also used to perform the identical task on the corresponding sections of the CAD file. The average of the variation in structural feature placement is 0.9% with an average standard deviation of ±0.68%. The average of the mismatch in structural feature area for the four layers is 1.37% with an average standard deviation ±0.99%. To aid in the visualization of the CAD / PZT comparison, the features of the CAD layer have been overlaid on top of the image of the sectioned PZT in Fig. 12. The structural deviation of the fabricated part from the

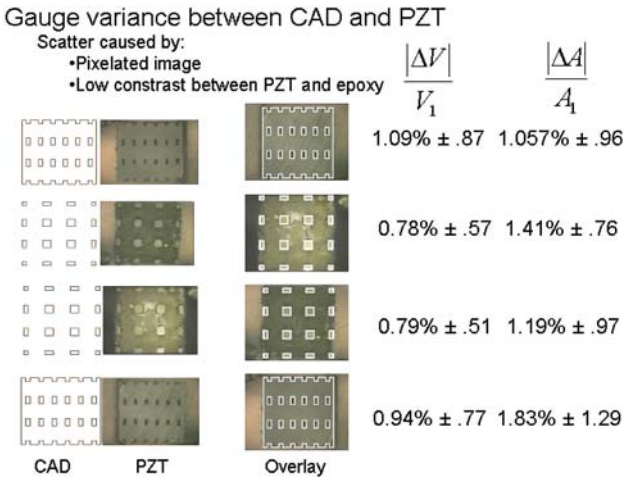

Fig. 12 Results of the fidelity analysis performed on the $3 \times 3 \times 1$ array of the 3d design 3 hydrophone structure. The feature areas and center points of the fabricated part are judged to be within 2% of the CAD file

CAD file in any layer is small, on the order of a few percent. This fabrication fidelity is comparable to tolerances obtained in many ceramic molding operations.

Conclusions

Complex three-dimensional designs for improved piezoelectric hydrophones, based on repeat units created Optimal Design methods. These designs can be realized in lead zirconate titanate piezoelectric ceramics using an indirect solid freeform fabrication technique employing lost molds to define internal void spaces. Lost molds were fabricated by wax-based ink jet deposition, and replicated in PZT ceramic using acrylate suspension polymerization. The physical size of the object is determined by the finest feature present in the design, and by the resolution of the ink jet device. Arrays with between 9 and 125 repeat units were fabricated with a fidelity of 0.9% in placement of features.

Acknowledgement This research was supported by the US National Science Foundation, under Grant 9972620.

References

1. Bendsøe MP, Kikuchi N (1988) Comput Methods Appl Mech Eng 71:197
2. Silva ECN (1998) Design of piezocomposite materials and piezoelectric transducers using topology optimization. Ph.D. Thesis, University of Michigan, Department of Mechanical Engineering and Applied Mechanics
3. Silva ECN, Fonseca JSO, Kikuchi N (1998) Comput Methods Appl Mech Eng 159:49
4. Silva ECN, Fonseca JSO, Kikuchi N (1997) Comput Mech 19(5):397
5. Sigmund O, Torquato S, Aksay IA (1998) J Mater Res 13(4):1038
6. Crumm T, Halloran JW, Silva ECN, Montero de Espinosa F (2006) J Mater Sci, doi:10.1007/s10853-006-1478-5
7. Xu Y (1991) Ferroelectric materials and their applications. North Holland-Elsevier Science, New York
8. Jaffe W, Cooke R, Jaffe H (1971) Piezoelectric ceramics. Academic Press, New York
9. Reilly CJ (2001) Novel electroactive ceramic architectures by indirect solid freeform fabrication. PhD Thesis, University of Michigan
10. Beaman JJ, Barlow JW et al (eds) (1997) Solid freeform fabrication: a new direction in manufacturing. Kluwer Academic Publishers, Boston MA
11. Miao W (2000) Fabrication of lead zirconate titanate actuator by suspension pollymerization casting. Ph.D. Thesis, University of Michigan
12. Bergstrom L (1994) In: Pugh RJ, Bergstrom L (eds) Surface and colloid chemistry in advanced ceramic processing. Marcel Dekker, New York, pp 193–239
13. Krieger IM, Dougherty TJ (1959) Transac Soc Reheol 3:137
14. Barnes H, Hutton J, Walters K (1989) In: Barnes H (ed) An introduction to rheology. Elsevier, New York, pp 115–139
15. Chu T-M, Halloran JW (2000) J Am Ceramic Soc 83(9):2189